The revival-collapse phenomenon in the quadrature squeezing and in the Wigner function of the single- mode field interacting with the two two-level atoms

2006 J. Phys. A: Math. Gen. 39 3397

(http://iopscience.iop.org/0305-4470/39/13/017)

INSTITUTE OF PHYSICS PUBLISHING JOURNAL OF PHYSICS A: MATHEMATICAL AND GENERAL

J. Phys. A: Math. Gen. **39** (2006) 3397–3410 doi:10.1088/0305-4470/39/13/017

The revival-collapse phenomenon in the quadrature squeezing and in the Wigner function of the single-mode field interacting with the two two-level atoms

Faisal A A El-Orany

Department of Mathematics and Computer Science, Faculty of Science, Suez Canal University, Ismailia, Egypt

Received 23 October 2005, in final form 27 January 2006
Published 15 March 2006
Online at stacks.iop.org/JPhysA/39/3397

Abstract

In this paper we consider a quantized single-mode field interacting with two two-level atoms. For the radiation field of this system we investigate the occurrence of the revival-collapse phenomenon in the evolution of the Wigner (W) function at the phase-space origin and of the quadrature squeezing. We show under certain conditions that the higher-order quadrature squeezing and the W function can provide complete information on the total atomic inversion. Moreover, we develop the notion of the geometric atomic inversion and show that it can be connected by the W function and the quadrature squeezing.

PACS numbers: 42.50.Dv, 42.60.Gd

1. Introduction

One of the most important models in quantum optics is the Jaynes–Cummings model (JCM) [1], which represents the interaction between a two-level atom and one quantized electromagnetic mode. The JCM has been experimentally realized in the framework of the Rydberg atom [2] and in the strong coupling regime [3]. In spite of its simplicity it provides a number of interesting phenomena such as the revival-collapse phenomenon (RCP) [4], sub-Poissonian photon statistics and squeezing [5]. The RCP is the most important one since it reflects the granular structure of the initial field distribution. At the fundamental level, the RCP reveals atom–field entanglement and it provides more information on the nonclassicality of the JCM. Also the revival results from the erasure of the atomic imprint onto the field and from the unitary deconstruction of the atom–field entanglement [6]. The generalization of the JCM either to many modes interacting with a single atom [7] or many atoms interacting with a single mode, e.g. [8], has been reported. Two two-level atoms interacting with a single-mode cavity field (TJCM) has taken much attention in the literature as a result of the progress in the quantum information [9]. More illustratively, the quantum entanglement criteria are basically given for two qubits, e.g. concurrence [10] and Peres–Horodecki measure [11].

Generally, for the TJCM there are different types of the atomic inversion, namely, single-atom inversions and total atomic inversion. The occurrence of the RCP in the evolution of these inversions has been investigated for the single-photon TJCM [12–14] as well as the multiphoton TJCM [15, 16]. Basically, the behaviour of the atomic inversions of the TJCM is completely different from that of the JCM since those of the former include a sum of harmonic functions, (i.e. cosines or sines), which oscillate at different frequencies providing RCP different from that of the latter. The RCP of the TJCM is quite sensitive to the ratio of the two transition dipole moments and to the photon statistics of the field [13]. In the framework of the two-atom Tavis–Cummings model the connection between the behaviour of the total atomic inversion, i.e. RCP, and the entanglement has been discussed [17].

Recently, we have shown that for the JCM there are relationships between the atomic inversion and each of the Wigner (W) function [7] and the quadrature squeezing [18–23]. Precisely, for the multimode multiphoton JCM the evolution of the W function at the phase-space origin—under certain conditions—provides complete information on the corresponding atomic inversion. Such behaviour is insensitive of the Kerr nonlinearity, the Stark shift effect, the types of the initial-field states and the atomic motion. On the other hand, it has been shown that for specific types of the initial-field states the quadrature squeezing can naturally exhibit the RCP as that of the corresponding atomic inversion. Furthermore, the evolution of the normal [18] and of the higher-order [19] squeezing of the three-photon JCM (with the field initially in the coherent state) can reflect the RCP involved in the $\langle\hat{\sigma}_z(T)\rangle$ of the standard, i.e. single-photon, JCM. Such types of relations are valid for any field whose photon-number distribution exhibits a smooth envelope, e.g. binomial state [23]. Apart from the standard JCM similar relations have been obtained for the intensity-dependent JCM [20], the two-photon JCM [21] and the two-mode JCM [22]. In the present paper, we study the occurrence of such a phenomenon for the cavity field of the TJCM. In other words, for the TJCM we study for the radiation field the possibility of involving the evolution of the W function at the phase-space origin and the quadrature squeezing information on the total atomic inversion. Needless to say that the treatment for the TJCM is more complicated than that for the single-atom JCM [18, 19]. In spite of this fact we obtain many interesting results. For instance, for this system we show that for particular types of initial states the quadrature squeezing can naturally involve complete information on the total atomic inversion. Furthermore, we show numerically that the information about the total atomic inversion of the single-photon and two-photon TJCM can be obtained from the evolution of the Nth-order quadrature squeezing of the three-photon and four-photon TJCM, respectively. This is quite similar to the single-atom JCM [19]. Moreover, we develop the notion of the geometric atomic inversion and prove that it can be obtained from the evolution of the W function as well as the quadrature squeezing. Also we show that under certain conditions there is a relationship between the total atomic inversion and W function. Actually, these results are interesting and motivated by two facts. (i)The TJCM is an important system since—beside the reasons given above—it is a subject of experiment. For instance, the analysis of a two-atom double-slit experiment based on environment-induced measurements is discussed in [24]. Furthermore, the generation of the entangled states from two two-level atoms inside a leakage optical cavity has been given in [25]. (ii) The results of the present paper are in the availability of the present technology. More illustratively, these results draw the attention to that the RCP of the TJCM can be measured by homodyne detectors [26], photon counting experiment [27], trapped ion technique [28, 29] and homodyne tomography [30, 31]. Some of these techniques have been already applied to the JCM. For instance, in the cavity QED, the homodyne detector technique has been applied to the single Rydberg atom and one-photon field for studying the field phase evolution of the regular JCM [32]. Quite recently the Rabi oscillations revival induced by time reversal has been observed using a

technique similar to that of the NMR refocusing [6]. Finally, for detecting the RCP produced by the TJCM the scheme given in [25] is more relevant: the system of two two-level atoms are placed inside a cavity with distance inbetween is much larger than the optical wavelength, and therefore dipole–dipole interaction can be neglected. The cavity mode is assumed to be resonant with the atomic transition frequency. The photons leaking from the cavity can be detected by a homodyne detector.

We perform such study in the following order: in section 2 we give the basic relations and equations for the system under consideration. Also we develop the definition of the geometric atomic inversion. In section 3 we investigate the evolution of the atomic inversion, the geometric atomic inversion and the W function at the phase-space origin, i.e. $W(0, T)$. In sections 4 and 5 we discuss the occurrence of the RCP in the quadrature squeezing naturally and numerically, respectively. In section 6 we summarize the main results. The appendix is given for deriving the re-scaled squeezing factors.

2. Basic equations and relations

In this section we give the basic relations and equations, which will be used in the paper. More precisely, we give the Hamiltonian of the system and derive its dynamical wavefunction. Also we evaluate the different forms of the atomic inversions as well as the W function at the phase-space origin. Also we give the definition of the Nth-order squeezing factors.

We start with developing the ℓ-photon coherent states [33–35] as

$$|\alpha\rangle = \sum_{n=0}^{\infty} C_n |ln\rangle, \tag{1}$$

where $C_n = \exp\left(-\frac{1}{2}|\alpha|^2\right)\frac{\alpha^n}{\sqrt{n!}}$ and l is a parameter, will be specified in the text. State (1) can cover a wide range of well-known states, i.e. when $l = 1$ and 2 it gives the coherent state and the two-photon coherent state, respectively.

In the rotating wave approximation the two-atom multiphoton single-mode Hamiltonian [12–16] is

$$\begin{aligned} &\frac{\hat{H}}{\hbar} = \hat{H}_0 + \hat{H}_I, \\ &\hat{H}_0 = \omega\hat{a}^\dagger\hat{a} + \omega_a\left(\hat{\sigma}_1^z + \hat{\sigma}_2^z\right), \qquad \hat{H}_I = \sum_{j=1}^{2}\lambda_j\left(\hat{a}^k\hat{\sigma}_j^+ + \hat{a}^{\dagger k}\hat{\sigma}_j^-\right), \end{aligned} \tag{2}$$

where $\hat{H}_0$ and $\hat{H}_I$ are the free and interaction parts of the Hamiltonian, $\hat{\sigma}_j^{\pm}$ and $\hat{\sigma}_j^z$ are the Pauli spin operators of the jth atom; $\hat{a}$ ($\hat{a}^\dagger$) is the annihilation (creation) operator denoting the cavity mode, ω and ω_a are the frequencies of the cavity mode and the atomic systems (we consider that the two atoms have the same frequency), λ_j is the atom–field coupling constant of the jth atom and k is the transition parameter. Throughout the investigation we assume that $\omega_a = 2k\omega$, (i.e. the exact resonance case) and the two atoms and field are initially in the excited atomic states $|+, +\rangle$ and the ℓ-photon coherent state, respectively. The atomic ground state is denoted by $|-\rangle$. From these facts the dynamical state of the whole system can be expressed in the following form:

$$\begin{aligned} |\Psi(T)\rangle = \sum_{n=0}^{\infty} C_n \left[X_1(T, n, k)|+, +, ln\rangle + X_2(T, n, k)|+, -, ln + k\rangle\right. \\ \left. + X_3(T, n, k)|-, +, ln + k\rangle + X_4(T, n, k)|-, -, ln + 2k\rangle\right]. \end{aligned} \tag{3}$$

In (3), without loss of generality, we have used the scaled time $T = \lambda_1 t$ instead of t. The explicit forms of the dynamical coefficients $X_j(T, n, k)$ can be obtained by solving the Schrödinger equation

$$\frac{\mathrm{i}}{\hbar}\frac{\partial}{\partial T}|\Psi(T)\rangle = \hat{H}_I|\Psi(T)\rangle. \tag{4}$$

From (3) and (4) we obtain a system of four first-order differential equations, which can be easily solved as

$$\begin{aligned}
X_1(T,n,k) &= \frac{1}{2\beta}\left[(\epsilon_2-\epsilon_1+\beta)\cos\left(\theta_n^{(1)}T\right)+(\epsilon_1-\epsilon_2+\beta)\cos\left(\theta_n^{(2)}T\right)\right],\\
X_2(T,n,k) &= \frac{-\mathrm{i}m\sqrt{\frac{(ln+k)!}{(ln)!}}}{2\beta}\left[D_+\frac{\sin\left(\theta_n^{(1)}T\right)}{\theta_n^{(1)}}-D_-\frac{\sin\left(\theta_n^{(2)}T\right)}{\theta_n^{(2)}}\right],\\
X_3(T,n,k) &= \frac{-\mathrm{i}\sqrt{\frac{(ln+k)!}{(ln)!}}}{2\beta}\left[d_+\frac{\sin\left(\theta_n^{(1)}T\right)}{\theta_n^{(1)}}-d_-\frac{\sin\left(\theta_n^{(2)}T\right)}{\theta_n^{(2)}}\right],\\
X_4(T,n,k) &= \frac{2m\sqrt{\frac{(ln+2k)!}{(ln)!}}}{\beta}\left[\cos\left(\theta_n^{(1)}T\right)-\cos\left(\theta_n^{(2)}T\right)\right],
\end{aligned} \tag{5}$$

where

$$\begin{aligned}
\epsilon_1 &= (1+m^2)\frac{(ln+2k)!}{(ln+k)!}, \qquad \epsilon_2 = (1+m^2)\frac{(ln+k)!}{(ln)!},\\
\beta &= \sqrt{(1+m^2)^2\left[\frac{(ln+2k)!}{(ln+k)!}-\frac{(ln+k)!}{(ln)!}\right]^2+16m^2\frac{(ln+2k)!}{(ln)!}},\\
\theta_n^{(1)} &= \frac{1}{\sqrt{2}}\sqrt{\epsilon_2+\epsilon_1+\beta}, \qquad \theta_n^{(2)} = -\frac{1}{\sqrt{2}}\sqrt{\epsilon_2+\epsilon_1-\beta},\\
D_\pm &= (1+m^2)\left[\frac{(ln+k)!}{(ln)!}-\frac{(ln+2k)!}{(ln+k)!}\right]+4\frac{(ln+2k)!}{(ln+k)!}\pm\beta,\\
d_\pm &= (1+m^2)\left[\frac{(ln+k)!}{(ln)!}-\frac{(ln+2k)!}{(ln+k)!}\right]+4m^2\frac{(ln+2k)!}{(ln+k)!}\pm\beta
\end{aligned} \tag{6}$$

and $m = \lambda_2/\lambda_1$. Throughout the paper the values $m = 1$ and $m \neq 1$ denote the symmetric and asymmetric cases, respectively. For the symmetric case the coefficients $X_j(T, n, k)$ take the forms:

$$\begin{aligned}
X_1(T,n,k) &= \frac{(ln)!(ln+k)!}{[(ln+k)!]^2+(ln)!(ln+2k)!}\left[\frac{(ln+k)!}{(ln)!}\cos(T\Theta_n)+\frac{(ln+2k)!}{(ln+k)!}\right],\\
X_2(T,n,k) &= X_3(T,n,k) = -\mathrm{i}\sqrt{\frac{(ln+k)!}{(ln)!}}\frac{\sin(T\Theta_n)}{\Theta_n},\\
X_4(T,n,k) &= \frac{(ln+k)!\sqrt{(ln)!(ln+2k)!}}{[(ln+k)!]^2+(ln)!(ln+2k)!}\left[\cos(T\Theta_n)-1\right],
\end{aligned} \tag{7}$$

where $\Theta_n = \sqrt{2\frac{(ln+k)!}{(ln)!}+2\frac{(ln+2k)!}{(ln+k)!}}$.

As we deal with the two atoms system we have different forms of the atomic inversions, namely, the first atom $\langle\sigma_1^z(T)\rangle$, the second atom $\langle\sigma_2^z(T)\rangle$ and the total atomic inversions $\langle\sigma_T^z(T)\rangle = \frac{1}{2}\left[\langle\sigma_1^z(T)\rangle+\langle\sigma_2^z(T)\rangle\right]$. Additionally, we develop the notion of the geometric atomic

inversion as $\langle\sigma_1^z(T)\sigma_2^z(T)\rangle$. The origin of using 'geometric' is in the similarity between this quantity and the geometric mean value, which for two c-numbers c_1, c_2 is $\sqrt{c_1c_2}$. The forms of these atomic inversions related to state (3) can be expressed as

$$\begin{aligned}
\langle\sigma_1^z(T)\rangle &= \sum_{n=0}^{\infty}|C_n|^2[|X_1(T,n,k)|^2+|X_2(T,n,k)|^2-|X_3(T,n,k)|^2-|X_4(T,n,k)|^2],\\
\langle\sigma_2^z(T)\rangle &= \sum_{n=0}^{\infty}|C_n|^2[|X_1(T,n,k)|^2-|X_2(T,n,k)|^2+|X_3(T,n,k)|^2-|X_4(T,n,k)|^2],\\
\langle\sigma_T^z(T)\rangle &= \sum_{n=0}^{\infty}|C_n|^2[|X_1(T,n,k)|^2-|X_4(T,n,k)|^2],\\
\langle\sigma_1^z(T)\sigma_2^z(T)\rangle &= \sum_{n=0}^{\infty}|C_n|^2[|X_1(T,n,k)|^2-|X_2(T,n,k)|^2-|X_3(T,n,k)|^2+|X_4(T,n,k)|^2].
\end{aligned} \tag{8}$$

One can easily realize for the symmetric case that $\langle\sigma_1^z(T)\rangle = \langle\sigma_2^z(T)\rangle = \langle\sigma_T^z(T)\rangle$.

On the other hand, the W function is an important quantity in quantum optics since it can be experimentally measured by several means, i.e. photon counting experiment [27], using a simple experiment similar to that used in the cavity QED and trapped ions [28, 29] and tomographic reconstruction from data obtained in homodyne measurements [30, 31]. Most of these techniques have been subjected to measure the phase-space origin of the W function [7], which can be obtained through the relation:

$$W(0,T) = \mathrm{Tr}[\hat{\rho}(T)\exp(\mathrm{i}\pi\hat{a}^\dagger\hat{a})], \tag{9}$$

where $\hat{\rho}(T)$ is the density matrix of the system under consideration. In (9) we have dropped the pre-factor $\frac{1}{\pi}$ from the definition of the W function since it does not affect the overall dynamical behaviour of the $W(0,T)$. It is evident from (9) that the main contribution in the $W(0,T)$ is coming from the diagonal terms of the density matrix of the system. This situation is similar to that of the atomic inversions (cf (8)). This indicates that there is a relationship between $W(0,T)$ and the atomic inversions. This issue will be discussed in the following section. Now from (3) and (9) we obtain

$$\begin{aligned}
W(0,T) = \sum_{n=0}^{\infty}|C_n|^2(-1)^{ln}[&|X_1(T,n,k)|^2+(-1)^k|X_2(T,n,k)|^2\\
&+(-1)^k|X_3(T,n,k)|^2+|X_4(T,n,k)|^2].
\end{aligned} \tag{10}$$

We close this section by defining the Nth-order quadrature squeezing operators as $\hat{X}_N = \frac{1}{2}(\hat{a}^N+\hat{a}^{\dagger N})$, $\hat{Y}_N = \frac{1}{2i}(\hat{a}^N-\hat{a}^{\dagger N})$, where N is a positive integer. The squeezing factors associated with $\hat{X}_N$ and $\hat{Y}_N$ can be, respectively, expressed as [36]:

$$\begin{aligned}
F_N(T) &= \langle\hat{a}^{\dagger N}(T)\hat{a}^N(T)\rangle + \mathrm{Re}\langle\hat{a}^{2N}(T)\rangle - 2(\mathrm{Re}\langle\hat{a}^N(T)\rangle)^2,\\
S_N(T) &= \langle\hat{a}^{\dagger N}(T)\hat{a}^N(T)\rangle - \mathrm{Re}\langle\hat{a}^{2N}(T)\rangle - 2(\mathrm{Im}\langle\hat{a}^N(T)\rangle)^2.
\end{aligned} \tag{11}$$

We use the present results in the following sections to find a relation between the different types of the atomic inversions and $W(0,T)$ as well as between the total atomic inversion and the quadrature squeezing.

3. Atomic inversion, geometric atomic inversion and the Wigner function

In this section we investigate the occurrence of the RCP in the evolution of the atomic inversions, geometric atomic inversion and the $W(0,T)$. Also we study the relations between

these quantities. Furthermore, performing such analysis is essential for the following sections, in which we deduce the relationship between the total atomic inversion and the quadrature squeezing.

First of all for the TJCM the quantities given in (8) can exhibit RCP only for $k = 1, 2$, provided that the intensity of the initial field is very strong, i.e. $\bar{n} = \langle \hat{n}(0) \rangle = l|\alpha|^2 \gg 1$. Throughout the paper we focus the attention on these cases. We start the investigation with the symmetric case when $(k, l) = (1, 1)$. In this case the initial photon-number distribution is Poissonian with sharp peak and hence the terms contributing effectively to the summations in (8) are those close to $n \simeq \bar{n}$. Thus the terms with the form $(1 + \eta'/n)$, where η' is a finite arbitrary number, tend to unity. This technique is called the strong-intensity regime (SIR). Therefore, from (8) the single-atom atomic inversion and the geometric atomic inversion, respectively, can be modified as

$$\langle \sigma_1^z(T) \rangle = \sum_{n=0}^{\infty} |C_n|^2 \cos\left(T\sqrt{2(2n+3)}\right), \tag{12}$$

$$\langle \sigma_1^z(T)\sigma_2^z(T) \rangle = \frac{1}{2} + \frac{1}{2}\sum_{n=0}^{\infty} |C_n|^2 \cos\left(2T\sqrt{2(2n+3)}\right). \tag{13}$$

It is evident that (13) is always non-negative since it is shifted from the origin by 0.5. Comparison between (12) and (13) shows that they can exhibit RCP but the revival patterns (revival amplitudes) of the latter are two times (half) greater than those of the former. From (12) and (13) one can deduce the connection between the atomic inversion and the geometric atomic inversion as

$$\langle \sigma_1^z(T)\sigma_2^z(T) \rangle = \tfrac{1}{2}\langle \sigma_1^z(2T) \rangle + \tfrac{1}{2}. \tag{14}$$

We have numerically checked the validity of (14) through the exact forms (8). For reasons that will be clear shortly, we deduce the asymptotic form for (12) by means of the SIR. In this case the square root in the argument of cosine in (12) can be modified as

$$\begin{aligned} \sqrt{2(2n+3)} &= 2\sqrt{\left(\bar{n} + \frac{3}{2}\right)}\left[1 + \frac{n - \bar{n}}{\left(\bar{n} + \frac{3}{2}\right)}\right]^{\frac{1}{2}}, \\ &\simeq \eta_1 + \eta_2 n, \end{aligned} \tag{15}$$

where

$$\eta_1 = \frac{\bar{n} + 3}{\sqrt{\bar{n} + \frac{3}{2}}}, \qquad \eta_2 = \frac{1}{\sqrt{\bar{n} + \frac{3}{2}}}. \tag{16}$$

The transition from the first line to the second line in (15) is done via Taylor's expansion with neglecting the higher-order terms, which are relatively small. On substituting (15) into (12) and after minor algebra we arrive at

$$\langle \sigma_1^z(T) \rangle \simeq \exp\left[-2|\alpha|^2 \sin^2\left(\frac{T}{2\eta_2}\right)\right] \cos[\eta_1 T + |\alpha|^2 \sin^2(T\eta_2)]. \tag{17}$$

In (17) the revival patterns occur when the exponential term has a maximum contribution, i.e. the revival time $T_r = \pi m'\sqrt{4\bar{n} + 6}$, where m' is integer. This form of T_r can be obtained also by estimating the time that neighbour terms in the sum are in phase. Similarly one can prove for $k = 2$ that $T_r = \pi$, which is typical with that of the single-atom JCM [5]. Also for (13) one can prove that the revival time is $T_r = 0.5\pi m'\sqrt{4\bar{n} + 6}$, i.e. it is one-half of (17).

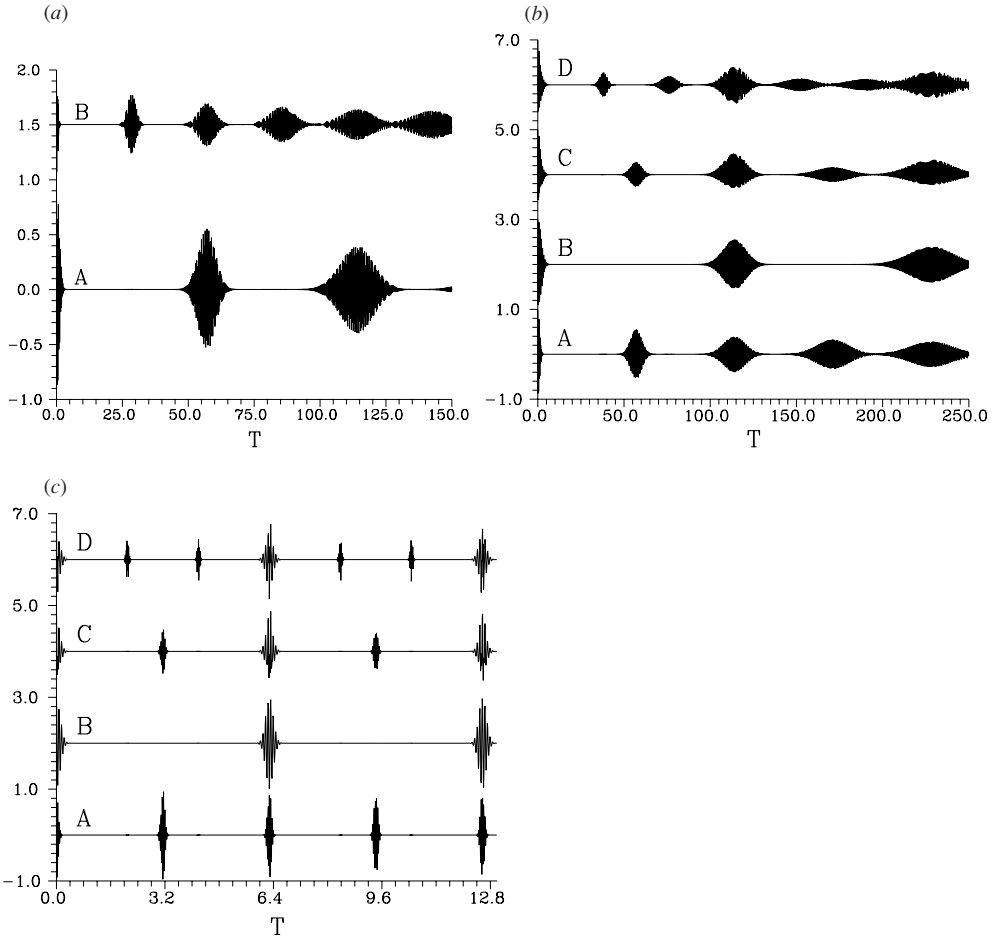

Figure 1. The different types of atomic inversions against the scaled time T for $\alpha = 9$. (a) for $(k, m) = (1, 1)$ $\langle\sigma_1^z(T)\rangle$ (curve A) and $\langle\sigma_1^z(T)\sigma_2^z(T)\rangle + 1$ (curve B). (b) for $(k, m) = (1, 0.5)$ $\langle\sigma_1^z(T)\rangle$ (curve A), $\langle\sigma_2^z(T)\rangle + 2$ (curve B), $\langle\sigma_T^z(T)\rangle + 4$ (curve C) and $\langle\sigma_1^z(T)\sigma_2^z(T)\rangle + 6$ (curve D). (c) the same as (b) but for $k = 2$.

These facts can be realized from figure 1, which are plotted for the exact forms of (8), for given values of the interaction parameters. It is obvious from figure 1(a) that for the symmetric case the behaviour is in a complete agreement with the analytical investigation given above. We turn the attention to the asymmetric case. From figure 1(b) the revival patterns occurring in the $\langle\sigma_1^z(T)\rangle$ are two times greater than those in the $\langle\sigma_2^z(T)\rangle$ (see curves A and B in figure 1(b)). This is related to the strengths of the interaction between the field and the two atoms, where the first-atom–field interaction is two times stronger than that of the second-atom–field interaction. Also we have checked the validity of this fact for $m = 0.25$. Now one can understand the asymmetry in the evolution of the $\langle\sigma_T^z(T)\rangle$ (see curve C in figure 1(b)), where it represents the sum of curves A and B in the same figure. To be more specific, when the revival patterns in curves A and B occur in the same interaction time domain, an amplified revival pattern appears in $\langle\sigma_T^z(T)\rangle$. Curve D in figure 1($b$) shows that $\langle\sigma_1^z(T)\sigma_2^z(T)\rangle$ exhibits RCP which is different from the other types. The remarks quoted to figure 1(b) are established for figure 1(c) of the

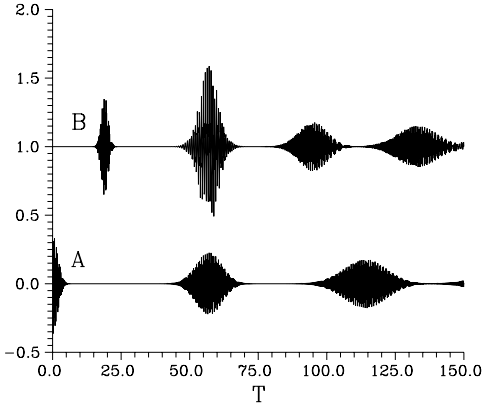

Figure 2. The evolution of the W function at the phase-space origin when $(k, l, \alpha) = (1, 1, 9)$ for $W(0, \tau)$ (curve A for $m = 1$) and $W(0, T) + 1$ (curve B for $m = 0.5$).

$k = 2$; however, for the latter the revival patterns are compact and systematic. Additionally, curve A in figure 1(c) is typical to that of the $\langle\sigma_T^z(T)\rangle$ for the symmetric case.

Now we draw the attention to the $W(0, T)$. From (10) one can easily realize that when k is even and l is even (odd) we obtain $W(0, T) = 1$ ($W(0, T) = -1$). This indicates that for these specific values of l and k the $W(0, T)$ is localized. Moreover, the evolution of the system with the initial odd parity states, e.g. odd coherent states, exhibits always nonclassical effects. On the other hand, when k is odd and l is even the expressions (8) and (10) lead to

$$W(0, T) = \langle\sigma_1^z(T)\sigma_2^z(T)\rangle. \tag{18}$$

Expression (18) indicates that for these particular values of k and l one can obtain information on the geometric atomic inversion of the TJCM by measuring the W function at the phase-space origin. As the main attention in the literature has been devoted to the TJCM when $m = k = l = 1$ we shed the light on the $W(0, T)$ of this case in a greater details. For this case the asymptotic form of the $W(0, T)$ (cf (10)) can be derived similarly as (17):

$$W(0, T) = \exp\left[-2|\alpha|^2\cos^2\left(\frac{T}{\eta_2}\right)\right]\cos[2\eta_1 T - |\alpha|^2\sin^2(2T\eta_2)]. \tag{19}$$

There is a kind of similarity between (17) and (19). From (19) the revival patterns can occur in the $W(0, T)$ when $T_r = \frac{h'\pi}{2}\eta_2$ where h' is odd integer. This indicates that the revival patterns occurring in the $W(0, T)$ are two times greater than those in $\langle\sigma_1^z(T)\rangle$ (cf (17)). Thus when $T \to \frac{1}{2}(\tau + \pi\eta_2)$ in (10) for $m = 1$, the $W(0, \tau)$ gives a complete information on the $\langle\sigma_1^z(T)\rangle$. This information is shown in figure 2 for given values of the interaction parameters. Comparison between curves A in figure 1(a) and figure 2 demonstrates our conclusion. Also curve B, which is given for the $W(0, T)$ of the asymmetric case, exhibits asymmetric RCP; however, it is different from those exhibited in the $\langle\sigma_T^z(T)\rangle$ and the $\langle\sigma_1^z(T)\sigma_2^z(T)\rangle$ (compare this curve with curves C and D in figure 1(b)).

4. Natural RCP in the quadrature squeezing

In this section for the TJCM we study the possibility of involving the quadrature squeezing information on the $\langle\sigma_T^z(T)\rangle$. This approach is based on the fact: $\hat{H}_0$ is a constant of motion, i.e. $\langle\hat{a}^\dagger\hat{a}\rangle$ and $\langle\sigma_T^z(T)\rangle$ can carry information on each others. For the sake of generality we study

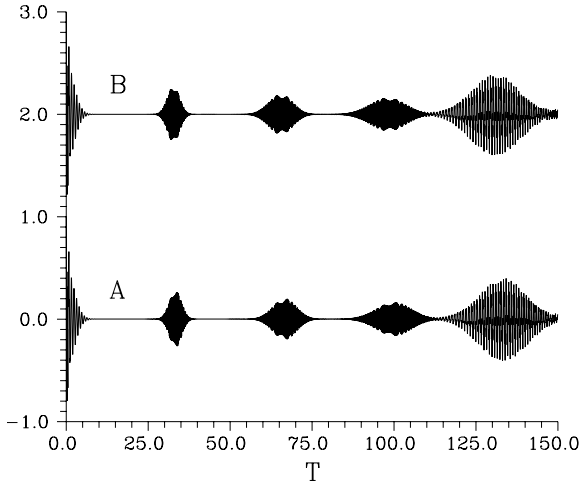

Figure 3. The total atomic inversion given by (23) (curve A for $N = 4$) and (8) (curve B) against the scaled time T for $(\alpha, l, k, m) = (9, 3, 1, 0.5)$. Curve B is shifted by 2.

the Nth-order squeezing. It is worth reminding that $\hat{a}^{\dagger N}\hat{a}^N + \sigma_T^z(T)$ is not a constant of motion; however, we show analytically and numerically that $\langle \hat{a}^{\dagger N}(T)\hat{a}^N(T)\rangle$ can give information on the $\langle \sigma_T^z(T)\rangle$. This occurs only for initial states which verify the condition $\langle \hat{a}^{s'}(T)\rangle = 0$ for all values of s'. Assume that the field is initially prepared in one of these states, then (11) reduces to

$$F_N(T) = S_N(T) = \langle \hat{a}^{\dagger N}(T)\hat{a}^N(T)\rangle, \tag{20}$$

where the expectation value $\langle \hat{a}^{\dagger N}(T)\hat{a}^N(T)\rangle$ can be evaluated as

$$\langle \hat{a}^{\dagger N}(T)\hat{a}^N(T)\rangle = \sum_{n=0}^{\infty} |C_n|^2 \left\{ \frac{(ln)!}{(ln-N)!}|X_1(T,n,k)|^2 + \frac{(ln+2k)!}{(ln+2k-N)!}|X_4(T,n,k)|^2 + \frac{(ln+k)!}{(ln+k-N)!}[|X_2(T,n,k)|^2 + |X_3(T,n,k)|^2] \right\}. \tag{21}$$

As a result of the complexity of the asymmetric case we restrict the analysis to the symmetric case, for which we obtain a general formula connecting the total atomic inversion to the Nth-order quadrature squeezing. Eventually we apply this formula to the asymmetric case. In doing so, we assume that the SIR is applicable and N is finite. For $k = 1$ the expression (21) can be rewritten as

$$\begin{aligned}\langle \hat{a}^{\dagger N}(T)\hat{a}^N(T)\rangle &= \langle \hat{a}^{\dagger N}(0)\hat{a}^N(0)\rangle + N\langle \hat{a}^{\dagger N-1}(0)\hat{a}^{N-1}(0)\rangle \\ &\quad - N\sum_{n=0}^{\infty} |C_n|^2 \frac{(ln)!}{(ln+1-N)!}\cos\left(T\sqrt{2(2ln+3)}\right) + \frac{1}{4}N(N-1) \\ &\quad \times \sum_{n=0}^{\infty} |C_n|^2 \frac{(ln)!}{(ln+1-N)!}\left\{ \frac{1}{2}\cos\left(2T\sqrt{2(2ln+3)}\right) \right. \\ &\quad \left. + \frac{3}{2} - 2\cos\left(T\sqrt{2(2ln+3)}\right) \right\}. \end{aligned} \tag{22}$$

In the last two lines of (22), the amplitude of the first cosine is four times smaller than that of the second cosine. In other words, the contribution of the first cosine is relatively small

compared to the second one and can be considered zero. This approximation is rigorous at this stage; however, it does not provide much effect on the last formula, which will be in a normalized form. Thus after minor algebra the $\langle\sigma_T^z(T)\rangle$ can be obtained from (22) through the relation

$$\langle\sigma_T^z(T)\rangle = \frac{\langle\hat{a}^{\dagger N}(0)\hat{a}^N(0)\rangle + N\langle\hat{a}^{\dagger N-1}(0)\hat{a}^{N-1}(0)\rangle + \frac{3}{8}N(N-1)\langle\hat{a}^{\dagger N-2}(0)\hat{a}^{N-2}(0)\rangle - S_N(T)}{N\langle\hat{a}^{\dagger N-1}(0)\hat{a}^{N-1}(0)\rangle + \frac{1}{2}N(N-1)\langle\hat{a}^{\dagger N-2}(0)\hat{a}^{N-2}(0)\rangle}. \tag{23}$$

Actually, we found that the expression (23) works well for the symmetric and asymmetric cases. In figure 3 we depict $\langle\sigma_T^z(T)\rangle$ for the asymmetric case of the fourth-order squeezing given by (23) (curve A). Also for the sake of comparison we plot the $\langle\sigma_T^z(T)\rangle$ given by (8) (curve B) for the same values of the interaction parameters. Comparison between the two curves is instructive and demonstrate our conclusion. On the other hand, there is a difficulty in deriving general formula for the case $k = 2$. Thus we provide the expression related to $N = 2$, i.e. the amplitude-squared squeezing, as

$$\langle\sigma_T^z(T)\rangle = \frac{\langle\hat{a}^{\dagger 2}(0)\hat{a}^2(0)\rangle + 4\langle\hat{a}^\dagger(0)\hat{a}(0)\rangle + 5 - S_2(T)}{4\langle\hat{a}^\dagger(0)\hat{a}(0)\rangle + 6}. \tag{24}$$

It is worth mentioning that the relation, which connects between $\langle\sigma_T^z(T)\rangle$ and normal squeezing for $k = 2$, is easy to be obtained. Moreover, we have numerically checked the validity of the formula (24).

5. Numerical RCP in the quadrature squeezing

In this section for the TJCM with $k > 2$ and the field initially in the coherent state we drive the Nth-order re-scaled squeezing factors, which can give information on the $\langle\sigma_T^z(T)\rangle_{k=1}$ and on the $\langle\sigma_T^z(T)\rangle_{k=2}$. More illustratively, we find the values of the transition parameter k for which the squeezing factors reduce to the $\langle\sigma_T^z(T)\rangle_{k=1}$ and $\langle\sigma_T^z(T)\rangle_{k=2}$. As we did in the previous section we derive the re-scaled squeezing factors for the symmetric case and hence apply them to the asymmetric one. It is obvious for real α that $\mathrm{Im}\langle\hat{a}^N(T)\rangle \simeq 0$. Thus the RCP (if it exists) can occur only in the $S_N(T)$ (cf (11)). Furthermore, when $k > 2$ the quantity $\langle\hat{a}^{\dagger N}(T)\hat{a}^N(T)\rangle$ exhibits chaotic behaviour and hence we can use $\langle\hat{a}^{\dagger N}(T)\hat{a}^N(T)\rangle \simeq \langle\hat{a}^{\dagger N}(0)\hat{a}^N(0)\rangle$. From this discussion one can easily realize that $\langle\hat{a}^{2N}(T)\rangle$ is responsible for the occurrence of the RCP in the $S_N(T)$. Therefore, we compare the expression of the $\langle\hat{a}^{2N}(T)\rangle$ to that of the $\langle\sigma_T^z(T)\rangle_{k=1}$ and $\langle\sigma_T^z(T)\rangle_{k=2}$ (see the appendix). In the framework of the SIR and from the information given in the appendix the Nth-order re-scaled squeezing factors are

$$Q_N(T) = \frac{\bar{n}^N - 2S_N(bT)}{\bar{n}^N}, \tag{25}$$

where

$$b = \begin{cases} \dfrac{1}{3N}, & \langle\sigma_T^z(T)\rangle_{k=1}, \\ \dfrac{1}{4N}, & \langle\sigma_T^z(T)\rangle_{k=2}. \end{cases} \tag{26}$$

As we have shown in the appendix that the quadrature squeezing can exhibit RCP similar to that of the $\langle\sigma_T^z(T)\rangle_{k=1}$ and $\langle\sigma_T^z(T)\rangle_{k=2}$ when $k = 3$ and $k = 4$, respectively. Surprisingly, these

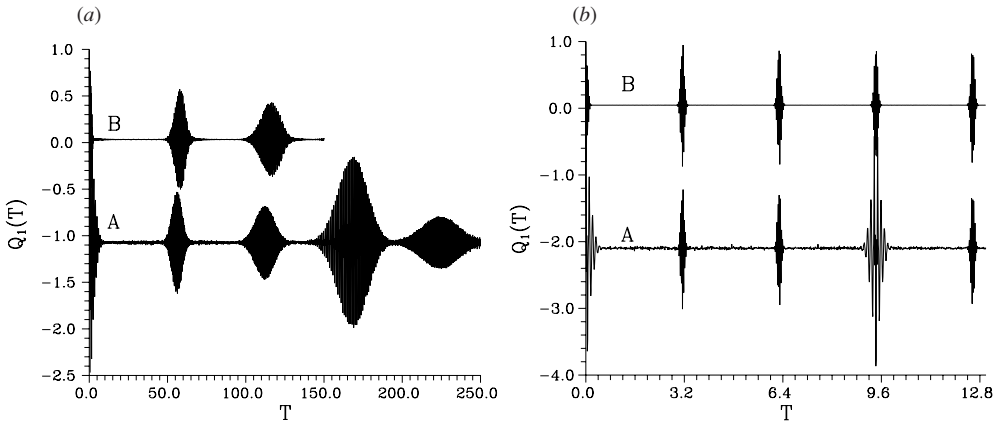

Figure 4. The re-scaled squeezing factor $Q_1(T)$ against the scaled time T when $(\alpha, l, N) = (9, 1, 1)$ for $k = 3$ (a) and 4 (b). Curves B and A are given for $m = 1$ and 0.5, respectively.

results are similar to those of the single-atom JCM [18–21]; however, here the situation is rather complicated.

Now we draw the attention to the asymmetric case. From the information given above one could expect that the behaviour of the asymmetric case will be quite similar to that of the symmetric case; however, the difficulty is to find the exact values of the parameter b. This problem can be numerically solved. Information on the re-scaled squeezing factors for the symmetric and asymmetric cases is shown in figure 4 for given values of the interaction parameters. Curves A in figures 4(a) and (b) belong to the asymmetric case, for which we have used $b = 0.46$ and 0.33, respectively. Comparison between curves B in figure 4 and the corresponding curves A in figures 1(a) and (c) shows that the formula (25) gives perfect information on the total atomic inversions of the symmetric case. Nevertheless, for the asymmetric case there are agreement and disagreement (compare curves A in figure 4 with the corresponding curves C in figure 1). For instance, there is a good agreement in the locations of the revival patterns in the interaction time domain; however, there is disagreement in the shapes of these patterns. Also one can note that these curves are shifted from zeros. Also we have checked (25) for $N = 2$ and arrived at the same conclusion.

We conclude this section by the following remark: information on the geometric atomic inversion can be obtained from the squeezing factors. This is quite obvious from the discussion given in section 3. Without much effort one can obtain the Nth-order squeezing factors, which give a complete information on the geometric atomic inversions for $m = 1$ as

$$Q'_N(T) = \frac{\bar{n}^N - S_N(b'T)}{\bar{n}^N}, \tag{27}$$

where

$$b' = \begin{cases} \dfrac{2}{3N}, & \left\langle \sigma_1^z(T)\sigma_2^z(T)\right\rangle_{k=1}, \\ \dfrac{1}{2N}, & \left\langle \sigma_1^z(T)\sigma_2^z(T)\right\rangle_{k=2}. \end{cases} \tag{28}$$

We have numerically checked the validity of (27).

6. Conclusion

In this paper we have investigated the system of two two-level atoms interacting with multiphoton single-mode field. The two atoms and the field are initially prepared in the excited atomic states and the ℓ-photon coherent state, respectively. The attention has been focused on the occurrence of the RCP in the evolution of the $W(0, T)$ and the quadrature squeezing and how these quantities can be connected by the corresponding atomic inversion. We have treated two cases, namely, symmetric and asymmetric based on the relation between the atom–field coupling constants. For this system we have developed the notion of the geometric atomic inversion and showed that it can be obtained from the $W(0, T)$ and the quadrature squeezing. Also we have shown under certain conditions that there is a relationship between the total atomic inversion and $W(0, T)$. We have proved for particular types of the initial states that the Nth-order quadrature squeezing can naturally involve information on the total atomic inversion. Also we have numerically shown that $\langle\sigma_T^z(T)\rangle_{k=1}$ $\left(\langle\sigma_T^z(T)\rangle_{k=2}\right)$ can be obtained from the Nth-order quadrature squeezing of the three-photon (four-photon) TJCM. For all these cases we have derived the re-scaled squeezing factors, which can provide complete information on the total atomic inversion. Also similar relations have been obtained for the geometric atomic inversion.

Acknowledgments

The author would like to thank the Abdus Salam International Centre for Theoretical Physics, Strada Costiers, 11 34014 Trieste Italy for the hospitality and financial support under the system of associateship, where a part of this work is done.

Appendix

In this appendix we derive the formula (25) by comparing the expression of the $\langle\hat{a}^{2N}(T)\rangle$ to that of the atomic inversion (12). In the SIR the quantity $\langle\hat{a}^{2N}(T)\rangle$ for the dynamical state (3) with $l = m = 1$ takes the form:

$$\langle\hat{a}^{2N}(T)\rangle = \bar{n}^N \sum_{n=0}^{\infty} |C_n|^2 [\zeta_1(n)\cos(T\Theta_{n+2N})\cos(T\Theta_n) + \zeta_2(n)\cos(T\Theta_{n+2N}) + \zeta_3(n)\cos(T\Theta_n) + \zeta_4(n)\sin(T\Theta_{n+2N})\sin(T\Theta_n) + \zeta_5(n)], \tag{A.1}$$

where the explicit forms of the coefficients $\zeta_j(n)$ can be easily derived. Here we give only the explicit form of the $\zeta_1(n)$ as

$$\zeta_1(n) = \frac{[(n+k)!(n+2N+k)!]^2 + n!(n+k)!(n+k+2N)!(n+2k+2N)!}{\{[(n+k)!]^2 + n!(n+2k)!\}\{[(n+k+2N)!]^2 + (n+2N)!(n+2k+2N)!\}}. \tag{A.2}$$

Now we evaluate the asymptotic form for $\zeta_1(n)$. This can be achieved by simplifying the factorials in (A.2) using the SIR. For instance, the factorial $(n+k)!$, say, can be rewritten as

$$(n+k)! = n!n^k \prod_{j=1}^{k} \left(1 + \frac{j}{n}\right). \tag{A.3}$$

For finite values of k and N the right-hand side of (A.3) reduces to $n!n^k$. Applying these procedures for all factorials in (A.2) leads to $\zeta_1(n) \simeq 1/2$. Similarly one can prove that

$\zeta_2(n) = \zeta_3(n) = 0$ and $\zeta_4(n) = \zeta_5(n) = 1/2$. Therefore, equation (A.1) can be simply written as

$$\langle \hat{a}^{2N}(T)\rangle = \frac{\bar{n}^N}{2} + \frac{\bar{n}^N}{2}\sum_{n=0}^{\infty}|C_n|^2\cos[T(\Theta_{n+2N} - \Theta_n)]. \tag{A.4}$$

The expression (A.4) can provide dynamical behaviour similar to that of (12) if the arguments of the cosines in the two expressions are comparable. Thus we seek the proportionality factor, μ_N, which can play this role. This factor, i.e. μ_N, can be obtained from the following expression:

$$\begin{aligned}\mu_N &= \frac{\Theta_{n+2N} - \Theta_n}{\sqrt{2(2n+3)}},\\ &= \frac{\frac{(n+2N+k)!}{(n+2N)!} - \frac{(n+k)!}{n!} + \frac{(n+2N+2k)!}{(n+2N+k)!} - \frac{(n+2k)!}{(n+k)!}}{\sqrt{2(2n+3)}\left[\sqrt{\frac{(n+2N+k)!}{(n+2N)!} + \frac{(n+2N+2k)!}{(n+2N+k)!}} + \sqrt{\frac{(n+k)!}{n!} + \frac{(n+2k)!}{(n+k)!}}\right]}.\end{aligned} \tag{A.5}$$

The first two terms in the numerator of (A.5) can be modified as

$$\frac{(n+2N+k)!}{(n+2N)!} - \frac{(n+k)!}{n!} = 2Nkn^{k-1} + n^{k-2}(..) + \cdots + n^0(..). \tag{A.6}$$

Similarly, the other two terms in the numerator of (A.5) can be treated. For denominator, one has to use procedure as that applied to (A.3). Substituting all these results in (A.5) one obtains

$$\mu_N \simeq \tfrac{1}{4}\left[4Nkn^{\frac{k-3}{2}} + n^{\frac{k-5}{2}}(..) + n^{\frac{k-7}{2}}(..) + \cdots\right]. \tag{A.7}$$

From (A.7) it is obvious that in the SIR the RCP involved in the $\langle\sigma_T^z(T)\rangle_{k=1}$ can occur in the quadrature squeezing of the multiphoton TJCM only when $k = 3$ and hence $\mu_N = 3N$. Similarly one can prove that the RCP in the $\langle\sigma_T^z(T)\rangle_{k=2}$ can occur in the quadrature squeezing of the multiphoton TJCM only when $k = 4$ with $\mu_N = 4N$. Finally, the calculations given in this appendix lead to the formula (25).

References

[1] Jaynes E T and Cummings F W 1963 *Proc. IEEE* **51** 89

[2] Kaluzny Y, Goy P, Gross M, Raimond J M and Haroche S 1983 *Phys. Rev. Lett.* **51** 1175
Rempe G, Walther H and Klein N 1987 *Phys. Rev. Lett.* **57** 353

[3] Boca A, Miller R, Birnbaum K M, Boozer A D, McKeever J and Kimble H J 2004 *Phys. Rev. Lett.* **93** 233603

[4] Eberly J H, Narozhny N B and Sanchez-Mondragon J J 1980 *Phys. Rev. Lett.* **44** 1323
Narozhny N B, Sanchez-Mondragon J J and Eberly J H 1981 *Phys. Rev.* A **23** 236
Yoo H I, Sanchez-Mondragon J J and Eberly J H 1981 *J. Phys. A: Math. Gen.* **14** 1383
Yoo H I and Eberly J H 1981 *Phys. Rep.* **118** 239

[5] El-Orany F A A and Obada A-S 2003 *J. Opt. B: Quant. Semiclas. Opt.* **5** 60

[6] Meunier T, Gleyzes S, Maioli P, Auffeves A, Nogues G, Brune M, Raimond J M and Haroche S 2005 *Phys. Rev. Lett.* **94** 010401

[7] El-Orany F A A 2004 *J. Phys. A: Math. Gen.* **37** 6157

[8] Kozierowski M, Mamedov A A and Chumakov S M 1990 *Phys. Rev.* A **42** 1762
Kozierowski M, Chumakov S M, Swiatlowski J and Mamedov A A 1992 *Phys. Rev.* A **46** 7220
Kozierowski M and Chumakov S M 1995 *Phys. Rev.* A **52** 4294
Chumakov S M, Klimov A B and Sanchez-Mondragon J J 1995 *Opt. Commun.* **118** 529

[9] Bennett C H 1995 *Phys. Today* **48** 24
Divincenzo D P 1995 *Science* **270** 255
Nielsen M A and Chuang I L 2000 *Quantum Computation and Quantum Information* (Cambridge: Cambridge University Press)
Benenti G, Casati G and Strini G 2004 *Principle of Quantum Computation and Information* (Singapore: World Scientific)

[10] Wootters W K 1998 *Phys. Rev. Lett.* **80** 2245
Hill S and Wootters W K 1997 *Phys. Rev. Lett.* **78** 5022
[11] Peres A 1996 *Phys. Rev. Lett.* **77** 1413
Horodecki P 1997 *Phys. Lett.* A **232** 333
[12] Iqbal M S, Mahmood S, Razmi M S K and Zubairy M S 1988 *J. Opt. Soc. Am.* B **5** 1312
[13] Sharma M P, Cardimona D A and Gavrielides A 1989 *J. Opt. Soc. Am.* B **6** 1942
[14] Jex I, Matsuoko M and Koashi M 1993 *Quant. Opt.* **5** 275
[15] Jex I 1990 *Quant. Opt.* **2** 443
[16] Abdel-Aty M 2004 *J. Opt. B: Quant. Semiclass. Opt.* **6**
[17] Tessier T E, Deutsch I H and Delgado A 2003 *Phys. Rev.* A **68** 062316
[18] El-Orany F A A 2004 *J. Phys. A: Math. Gen.* **37** 9037
[19] El-Orany F A A 2005 *J. Phys. A: Math. Gen.* **38** 5557
[20] El-Orany F A A 2006 *J. Mod. Opt.* at press
[21] El-Orany F A A 2006 *Opt. Commun.* at press
[22] El-Orany F A A 2005 *J. Opt. B: Quant. Semiclass. Opt.* **7** 341
[23] El-Orany F A A 2006 *Phys. Lett.* A submitted
[24] Schön C and Beige A 2001 *Phys. Rev.* A **64** 023806
[25] Plenio M B, Huelga S F, Beige A and Knight P L 1999 *Phys. Rev.* A **59** 2468
Yi X X, Yu C S, Zhou L and Song H S 2003 *Phys. Rev.* A **68** 052304
[26] Mandel L and Wolf E 1995 *Optical Coherence and Quantum Optics* (Cambridge: Cambridge University Press)
Leonhardt U 1997 *Measuring the Quantum State of Light* (Cambridge: Cambridge University Press)
[27] Banaszek K and Wódkiewicz k 1996 *Phys. Rev. Lett.* **76** 4344
Wallentowitz S and Vogel W 1996 *Phys. Rev.* A **53** 4528
[28] Lutterbach L G and Davidovich L 1997 *Phys. Rev. Lett.* **78** 2547
[29] Nogues G, Rauschenbeutel A, Osnaghi S, Bertet P, Brune M, Raimond J M, Haroche S, Lutterbach L G and Davidovich L 2000 *Phys. Rev.* A **62** 054101
[30] Vogel K and Risken H 1989 *Phys. Rev.* A **40** 2847
[31] Beck M, Smithey D T and Raymer M G 1993 *Phys. Rev.* A **48** 890
Smithey D T, Beck M, Cooper J and Raymer M G 1993 *Phys. Rev.* A **48** 3159
Beck M, Smithey D T, Cooper J and Raymer M G 1993 *Opt. Lett.* **18** 1259
Smithey D T, Beck M, Cooper J, Raymer M G and Faridani M B A 1993 *Phys. Scr.* T **48** 35
[32] Rauschenbeutel A, Nogues G, Osnaghi S, Bertet P, Brune M, Raimond J M and Haroche S 1999 *Phys. Rev. Lett.* **83** 5166
Raimond J M, Brune M and Haroche S 2001 *Rev. Mod. Phys.* **73** 565
Bertet P, Auffeves A, Maioli P, Osnaghi S, Meunier T, Brune M, Raimond J M and Haroche S 2002 *Phys. Rev. Lett.* **89** 200402
[33] D'Ariano G, Rasetti M and Vadacchio M 1985 *Phys. Rev.* D **32** 1034
Katriel J, Solomon A, D'Ariano G and Rasetti M 1986 *Phys. Rev.* D **34** 332
D'Ariano G and Sterpi N 1989 *Phys. Rev.* A **39** 1810
[34] Bužek V and Jex I 1990 *Phys. Rev.* A **41** 4079
[35] Brandt R A and Greenberg O W 1969 *J. Math. Phys.* **10** 1168
[36] Hong C K and Mandel L 1985 *Phys. Rev.* A **32** 974
Hong C K and Mandel L 1985 *Phys. Rev. Lett.* **54** 323
Zhung Z-M, Xu L, Chui J-L and Li F-L 1990 *Phys. Lett.* A **150** 27